

Research Article

Radar Sensor Networks: Algorithms for Waveform Design and Diversity with Application to ATR with Delay-Doppler Uncertainty

Qilian Liang

Department of Electrical Engineering, University of Texas at Arlington, Room 518, 416 Yates Street, Arlington, TX 76019-0016, USA

Received 30 May 2006; Revised 28 November 2006; Accepted 29 November 2006

Recommended by Xiuzhen Cheng

Automatic target recognition (ATR) in target search phase is very challenging because the target range and mobility are not yet perfectly known, which results in delay-Doppler uncertainty. In this paper, we firstly perform some theoretical studies on radar sensor network (RSN) design based on linear frequency modulation (LFM) waveform: (1) the conditions for waveform coexistence, (2) interferences among waveforms in RSN, (3) waveform diversity in RSN. Then we apply RSN to ATR with delay-Doppler uncertainty and propose maximum-likelihood (ML) ATR algorithms for fluctuating targets and nonfluctuating targets. Simulation results show that our RSN vastly reduces the ATR error compared to a single radar system in ATR with delay-Doppler uncertainty. The proposed waveform design and diversity algorithms can also be applied to active RFID sensor networks and underwater acoustic sensor networks.

Copyright © 2007 Qilian Liang. This is an open access article distributed under the Creative Commons Attribution License, which permits unrestricted use, distribution, and reproduction in any medium, provided the original work is properly cited.

1. INTRODUCTION AND MOTIVATION

The goal for any target recognition system is to give the most accurate interpretation of what a target is at any given point in time. There are two classes of motion models of targets, one for maneuvering targets and one for nonmaneuvering (constant velocity and acceleration) targets. The area that is still lacking in target recognition is the ability to detect reliably when a target is beginning a maneuver where its speed and range are uncertain. The tracking system can switch the algorithms applied to the problem from a nonmaneuvering set to the maneuvering set when a target is beginning a maneuver. But when the tracker does finally catch up to the target after the maneuver and then perform ATR, the latency is too high. In time-critical mission situation, such latency in ATR is not tolerable. In this paper, we are interested in studying automatic target recognition with range and speed uncertainty, that is, delay-Doppler uncertainty, using radar sensor networks (RSN). The network of radar sensors should operate with multiple goals managed by an intelligent platform network that can manage the dynamics of each radar to meet the common goals of the platform rather than each radar to operate as an independent system. Therefore, it is significant

to perform signal design and processing and networking cooperatively within and between platforms of radar sensors and their communication modules. In this paper, we are interested in studying algorithms on radar sensor network (RSN) design based on linear frequency modulation (LFM) waveform: (1) the conditions for waveform coexistence, (2) interferences among waveforms in RSN, (3) waveform diversity in RSN. Then we apply RSN to automatic target recognition (ATR) with delay-Doppler uncertainty.

In nature, diverse waveforms are transmitted by animals for specific applications. For example, when a bat and a whale are in the search mode for food, they emit a different type of waveform than when they are trying to locate their prey. The Doppler-invariant waveforms that they transmit are environment dependent [1]. Hence, in RSN, it may be useful to transmit different waveforms from different neighbor radars and they can collaboratively perform waveforms diversity for ATR. Sowelam and Tewfik [2] developed a signal selection strategy for radar target classification, and a sequential classification procedure was proposed to minimize the average number of necessary signal transmissions. Intelligent waveform selection was studied in [3, 4], but the effect of Doppler shift was not considered. In [5], the performance of constant

frequency (CF) and LFM waveform fusion from the standpoint of the whole system was studied, but the effects of clutter were not considered. In [6], CF and LFM waveforms were studied for sonar system, but it was assumed that the sensor is nonintelligent (i.e., waveform cannot be selected adaptively). All the above studies and design methods were focused on the waveform design or selection for a single active radar or sensor. In [7], cross-correlation properties of two radars are briefly mentioned and the binary coded pulses using simulated annealing [8] are highlighted. However, the cross-correlation of two binary sequences such as binary coded pulses (e.g., Barker sequence) are much easier to study than that of two analog radar waveforms. In [9], CF waveform design was applied to RSN with application to ATR without any delay-Doppler uncertainty. In this paper, we will focus on the waveform design fusion for radar sensor networks using LFM waveform.

The rest of this paper is organized as follows. In Section 2, we study the coexistence of LFM radar waveforms. In Section 3, we analyze the interferences among LFM radar waveforms. In Section 4, we propose a RAKE structure for waveform diversity combining and propose maximum-likelihood (ML) algorithms for ATR with delay-Doppler uncertainty. In Section 5, we provide simulation results on ML-ATR with delay-Doppler uncertainty. In Section 6, we conclude this paper and provide some future works.

2. COEXISTENCE OF LFM RADAR WAVEFORMS

In RSN, radar sensors will interfere with each other and the signal-to-interference-ratio may be very low if the waveforms are not properly designed. We will introduce orthogonality as one criterion for waveforms design in RSN to make them coexistence. Besides, the radar channel is narrowband, so we will also consider the bandwidth constraint.

In our radar sensor networks, we choose LFM waveform. The LFM waveform can be defined as

$$x(t) = \sqrt{\frac{E}{T}} \exp(j2\pi\beta t^2), \quad -\frac{T}{2} \leq t \leq \frac{T}{2}. \quad (1)$$

In radar, ambiguity function (AF) is an analytical tool for waveform design and analysis that succinctly characterizes the behavior of a waveform paired with its matched filter. The ambiguity function is useful for examining resolution, side lobe behavior, and ambiguities in both range and Doppler for a given waveform [10]. For a single radar, the matched filter for waveform $x(t)$ is $x^*(-t)$, and the ambiguity function of LFM waveform is [10]

$$\begin{aligned} A(\tau, F_D) &= \left| \int_{-T/2+\tau}^{T/2} x(t) \exp(j2\pi F_D t) x^*(t-\tau) dt \right| \\ &= \left| \frac{E \sin[\pi(F_D + \beta\tau)(T - |\tau|)]}{T\pi(F_D + \beta\tau)} \right|, \quad -T \leq \tau \leq T. \end{aligned} \quad (2)$$

Three special cases can simplify this AF:

(1) when $\tau = 0$,

$$A(0, F_D) = \left| \frac{E \sin(\pi F_D T)}{T\pi(F_D)} \right|; \quad (3)$$

(2) when $F_D = 0$,

$$A(\tau, 0) = \left| \frac{E \sin[\pi\beta\tau(T - |\tau|)]}{T\pi\beta\tau} \right|, \quad -T \leq \tau \leq T; \quad (4)$$

(3) and

$$A(0, 0) = E. \quad (5)$$

However, the above ambiguity is for one radar only (no co-existing radar).

For radar sensor networks, the waveforms from different radars will interfere with each other. We choose the waveform for radar i as

$$x_i(t) = \sqrt{\frac{E}{T}} \exp[j2\pi(\beta t^2 + \delta_i t)], \quad -\frac{T}{2} \leq t \leq \frac{T}{2} \quad (6)$$

which means there is a frequency shift δ_i for radar i . To minimize the interference from one waveform to the other, optimal values for δ_i should be determined to have the waveforms orthogonal to each other, that is, let the cross-correlation between $x_i(t)$ and $x_n(t)$ be 0,

$$\begin{aligned} &\int_{-T/2}^{T/2} x_i(t) x_n^*(t) dt \\ &= \frac{E}{T} \int_{-T/2}^{T/2} \exp[j2\pi(\beta t^2 + \delta_i t)] \exp[-j2\pi(\beta t^2 + \delta_n t)] dt \\ &= E \operatorname{sinc}[\pi(\delta_i - \delta_n)T]. \end{aligned} \quad (7)$$

If we choose

$$\delta_i = \frac{i}{T}, \quad (8)$$

where i is a dummy index, then (7) can have two cases:

$$\int_{-T/2}^{T/2} x_i(t) x_n^*(t) dt = \begin{cases} E, & i = n, \\ 0, & i \neq n. \end{cases} \quad (9)$$

So, choosing $\delta_i = i/T$ in (6) can have orthogonal waveforms, that is, the waveforms can coexist if the carrier spacing is $1/T$ between two radar waveforms. That is, orthogonality amongst carriers can be achieved by separating the carriers by an integer multiple of the inverse of waveform pulse duration. With this design, all the orthogonal waveforms can work simultaneously. However, there may exist time delay and Doppler shift ambiguity which will have interferences to other waveforms in RSN.

3. INTERFERENCES OF LFM WAVEFORMS IN RADAR SENSOR NETWORKS

3.1. RSN with two radar sensors

We are interested in analyzing the interference from one radar to another if there exist time delay and Doppler shift. For a simple case where there are two radar sensors (i and n), the ambiguity function of radar i (considering interference from radar n) is

$$A_i(t_i, t_n, F_{D_i}, F_{D_n}) \quad (10)$$

$$= \left| \int_{-\infty}^{\infty} [x_i(t) \exp(j2\pi F_{D_i} t) + x_n(t-t_n) \exp(j2\pi F_{D_n} t)] x_i^*(t-t_i) dt \right| \quad (11)$$

$$\leq \left| \int_{-T/2+\max(t_i, t_n)}^{T/2+\min(t_i, t_n)} x_n(t-t_n) \exp(j2\pi F_{D_n} t) x_i^*(t-t_i) dt \right| + \left| \int_{-T/2+t_i}^{T/2} x_i(t) \exp(j2\pi F_{D_i} t) x_i^*(t-t_i) dt \right| \quad (12)$$

$$= \left| \int_{-T/2+\max(t_i, t_n)}^{T/2+\min(t_i, t_n)} x_n(t-t_n) \exp(j2\pi F_{D_n} t) x_i^*(t-t_i) dt \right| + \left| \frac{E \sin[\pi(F_{D_i} + \beta t_i)(T - |t_i|)]}{T\pi(F_{D_i} + \beta t_i)} \right|. \quad (13)$$

To make analysis easier, we assume $t_i = t_n = \tau$ which is a reasonable assumption because radar sensors can be coordinated by the clusterhead to send out LFM waveforms. Then (13) can be simplified as

$$A_i(\tau, F_{D_i}, F_{D_n}) \approx |E \operatorname{sinc}[\pi(n-i+F_{D_n}T)]| + \left| \frac{E \sin[\pi(F_{D_i} + \beta\tau)(T - |\tau|)]}{T\pi(F_{D_i} + \beta\tau)} \right|. \quad (14)$$

Some special cases of (14) are listed as follows.

(1) If $F_{D_i} = F_{D_n} = 0$, then (14) becomes

$$A_i(\tau, 0, 0) \approx \left| \frac{E \sin[\pi\beta\tau(T - |\tau|)]}{\pi\beta T\tau} \right|. \quad (15)$$

(2) If $\tau = 0$, then (14) becomes

$$A_i(0, F_{D_i}, F_{D_n}) \approx |E \operatorname{sinc}[\pi(n-i+F_{D_n}T)]| + |E \operatorname{sinc}(\pi F_{D_i} T)|. \quad (16)$$

(3) If $F_{D_i} = F_{D_n} = 0$, $\tau = 0$, and δ_i and δ_n follow (8), then (14) becomes

$$A_i(0, 0, 0) \approx E. \quad (17)$$

3.2. RSN with M radar sensors

It can be extended to an RSN with M radars. Assuming time delay τ for each radar is the same, then the ambiguity function of radar 1 (considering interferences from all the other $M-1$ radars with CF pulse waveforms) can be expressed as

$$A_1(\tau, F_{D_1}, \dots, F_{D_M}) \approx \left| \sum_{i=2}^M E \operatorname{sinc}[\pi(i-1+F_{D_i}T)] \right| + \left| \frac{E \sin[\pi(F_{D_1} + \beta\tau)(T - |\tau|)]}{T\pi(F_{D_1} + \beta\tau)} \right|. \quad (18)$$

Similarly, we can have three special cases.

(1) If $F_{D_1} = F_{D_2} = \dots = F_{D_M} = 0$, then (18) becomes

$$A_1(\tau, 0, 0, \dots, 0) \approx \left| \frac{E \sin[\pi\beta\tau(T - |\tau|)]}{\pi\beta T\tau} \right|. \quad (19)$$

Comparing it against (4), it shows that our derived condition in (6) can have a radar in RSN and it gets the same signal strength as that of a single radar (no coexisting radar) when the Doppler shift is 0.

(2) If $\tau = 0$, then (18) becomes

$$A_1(0, F_{D_1}, F_{D_2}, \dots, F_{D_M}) \approx \left| \sum_{i=1}^M E \operatorname{sinc}[\pi(i-1+F_{D_i}T + \beta\tau T)] \right|. \quad (20)$$

Comparing to (3), a radar in RSN has more interferences when unknown Doppler shifts exist.

(3) If $F_{D_1} = F_{D_2} = \dots = F_{D_M} = 0$, $\tau = 0$, and δ_i in (6) follows (8), then (18) becomes

$$A_1(0, 0, 0, \dots, 0) \approx E. \quad (21)$$

4. APPLICATION TO ATR WITH DELAY-DOPPLER UNCERTAINTY

In RSN, the radar sensors are networked together in an ad hoc fashion. They do not rely on a pre-existing fixed infrastructure, such as a wireline backbone network or a base station. They are self-organizing entities that are deployed on demand in support of various events surveillance, battlefield, disaster relief, search and rescue, and so forth. Scalability concern suggests a hierarchical organization of radar sensor networks with the lowest level in the hierarchy being a cluster. As argued in [11–14], in addition to helping with scalability and robustness, aggregating sensor nodes into clusters has additional benefits:

- (1) conserving radio resources such as bandwidth;
- (2) promoting spatial code reuse and frequency reuse;
- (3) simplifying the topology, for example, when a mobile radar changes its location, it is sufficient for only the nodes in attended clusters to update their topology information;

- (4) reducing the generation and propagation of routing information; and,
 (5) concealing the details of global network topology from individual nodes.

In RSN, each radar can provide their waveform parameters such as δ_i to their clusterhead radar, and the clusterhead radar can combine the waveforms from its cluster members.

In RSN with M radars, the received signal for clusterhead (assume it is radar 1) is

$$r_1(u, t) = \sum_{i=1}^M \alpha(u) x_i(t - t_i) \exp(j2\pi F_{D_i} t) + n(u, t), \quad (22)$$

where $\alpha(u)$ stands for radar cross section (RCS) and can be modeled using nonzero constants for nonfluctuating target and four Swerling target models for fluctuating target [10]; F_{D_i} is the Doppler shift of target relative to waveform i ; t_i is delay of waveform i , and $n(u, t)$ is additive white Gaussian noise (AWGN). In this paper, we propose a RAKE structure for waveform diversity combining, as illustrated by Figure 1.

According to this structure, the received $r_1(u, t)$ is processed by a bank of matched filters, then the output of branch 1 (after integration) is

$$\begin{aligned} & |Z_1(u; t_1, \dots, t_M, F_{D_1}, \dots, F_{D_M})| \\ &= \left| \int_{-T/2}^{T/2} r_1(u, t) x_1^*(t - t_1) ds \right| \\ &= \left| \int_{-T/2}^{T/2} \left[\sum_{i=1}^M \alpha(u) x_i(t - t_i) \exp(j2\pi F_{D_i} t) + n(u, t) \right] \right. \\ &\quad \left. \times x_1^*(t - t_1) dt \right|, \end{aligned} \quad (23)$$

where $\int_{-T/2}^{T/2} n(u, t) x_1^*(t - t_1) dt$ can easily be proved to be AWGN, let

$$n(u, t_1) \triangleq \int_{-T/2}^{T/2} n(u, t) x_1^*(t - t_1) dt \quad (24)$$

follow a white Gaussian distribution. Assuming $t_1 = t_2 = \dots = t_M = \tau$, then based on (18),

$$\begin{aligned} & |Z_1(u; \tau, F_{D_1}, \dots, F_{D_M})| \\ &\approx \left| \sum_{i=2}^M \alpha(u) E \operatorname{sinc}[\pi(i - 1 + F_{D_i} T)] \right. \\ &\quad \left. + \frac{\alpha(u) E \sin[\pi(F_{D_1} + \beta\tau)(T - |\tau|)]}{T\pi(F_{D_1} + \beta\tau)} + n(u, \tau) \right|. \end{aligned} \quad (25)$$

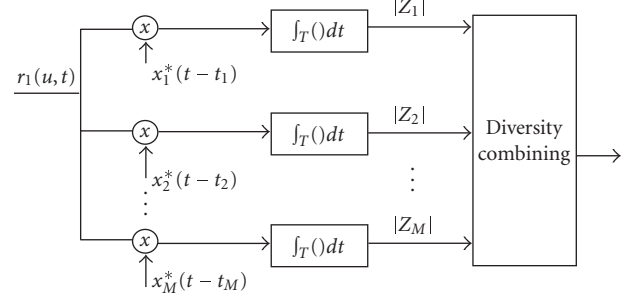


FIGURE 1: Waveform diversity combining by clusterhead in RSN.

Similarly, we can get the output for any branch m ($m = 1, 2, \dots, M$),

$$\begin{aligned} & |Z_m(u; \tau, F_{D_1}, \dots, F_{D_M})| \\ &\approx \left| \sum_{i=1, i \neq m}^M \alpha(u) E \operatorname{sinc}[\pi(i - m + F_{D_i} T)] \right. \\ &\quad \left. + \frac{\alpha(u) E \sin[\pi(F_{D_m} + \beta\tau)(T - |\tau|)]}{T\pi(F_{D_m} + \beta\tau)} + n(u, \tau) \right|. \end{aligned} \quad (26)$$

So, $|Z_m(u; \tau, F_{D_1}, \dots, F_{D_M})|$ consists of three parts, signal (reflected signal from radar m waveform):

$$\left| \frac{\alpha(u) E \sin[\pi(F_{D_m} + \beta\tau)(T - |\tau|)]}{T\pi(F_{D_m} + \beta\tau)} \right|, \quad (27)$$

interferences from other waveforms:

$$\sum_{i=1, i \neq m}^M |\alpha(u) E \operatorname{sinc}[\pi(i - m + F_{D_i} T)]|, \quad (28)$$

and noise: $|n(u, \tau)|$. Delay-Doppler uncertainty happens quite often in target search and recognition where target range and velocity are not yet perfectly known.

We can also have three special cases for

$$|Z_m(u; \tau, F_{D_1}, \dots, F_{D_M})|. \quad (29)$$

- (1) When $F_{D_1} = \dots = F_{D_M} = 0$,

$$\begin{aligned} & |Z_m(u; \tau, 0, 0, \dots, 0)| \\ &\approx \left| \frac{\alpha(u) E \sin[\pi\beta\tau(T - |\tau|)]}{T\pi\beta\tau} + n(u, \tau) \right|. \end{aligned} \quad (30)$$

- (2) If $\tau = 0$, then (26) becomes

$$\begin{aligned} & |Z_m(u; 0, F_{D_1}, \dots, F_{D_M})| \\ &\approx \left| \sum_{i=1}^M \alpha(u) E \operatorname{sinc}[\pi(i - m + F_{D_i} T)] + n(u) \right|. \end{aligned} \quad (31)$$

- (3) If $\tau = 0$ and $F_{D_1} = \dots = F_{D_M} = 0$, then (26) becomes

$$|Z_m(u; 0, 0, 0, \dots, 0)| \approx |E\alpha(u) + n(u)|. \quad (32)$$

How to combine all the Z_m 's ($m = 1, 2, \dots, M$) is very similar to the diversity combining in communications to combat channel fading, and the combination schemes may be different for different applications. In this paper, we are interested in applying RSN waveform diversity to ATR, for example, recognition that the echo on a radar display is that of an aircraft, ship, motor vehicle, bird, person, rain, chaff, clear-air turbulence, land clutter, sea clutter, bare mountains, forested areas, meteors, aurora, ionized media, or other natural phenomena. Early radars were "blob" detectors in that they detected the presence of a target and gave its location in range and angle, and radar began to be more than a blob detector and could provide recognition of one type of target from another [7]. It is known that small changes in the aspect angle of complex (multiple scatter) targets can cause major changes in the radar cross section (RCS). This has been considered in the past as a means of target recognition, and is called *fluctuation of radar cross section with aspect angle*, but it has not had much success [7]. In this paper, we propose a maximum-likelihood automatic target recognition (ML-ATR) algorithm for RSN. We will study both fluctuating targets and nonfluctuating targets.

4.1. ML-ATR for fluctuating targets with delay-Doppler uncertainty

Fluctuating target modeling is more realistic in which the target RCS is drawn from either the Rayleigh or chi-square of degree four pdf. The Rayleigh model describes the behavior of a complex target consisting of many scatters, none of which is dominant. The fourth-degree chi-square models targets having many scatters of similar strength with one dominant scatter. Based on different combinations of pdf and decorrelation characteristics (scan-to-scan or pulse-to-pulse decorrelation), four Swerling models are used [10]. In this paper, we will focus on "Swerling 2" model which is Rayleigh distribution with pulse-to-pulse decorrelation. The pulse-to-pulse decorrelation implies that each individual pulse results in an independent value for RCS α .

For Swerling 2 model, the RCS $|\alpha(u)|$ follows Rayleigh distribution and its I and Q subchannels follow zero-mean Gaussian distributions with variance γ^2 . Assume

$$\alpha(u) = \alpha_I(u) + j\alpha_Q(u) \quad (33)$$

and $n(u) = n_I(u) + jn_Q(u)$ follows zero-mean complex Gaussian distribution with variance σ^2 for the I and Q subchannels. Observe (26), for given τ, F_{D_i} ($i = 1, \dots, M$),

$$\begin{aligned} & \sum_{i=1, i \neq m}^M \alpha(u) E \operatorname{sinc} [\pi(i - m + F_{D_i} T)] \\ & + \frac{\alpha(u) E \sin [\pi(F_{D_m} + \beta\tau)(T - |\tau|)]}{T\pi(F_{D_m} + \beta\tau)} \\ & = \alpha(u) E \left[\sum_{i=1, i \neq m}^M \operatorname{sinc} [\pi(i - m + F_{D_i} T)] \right. \\ & \quad \left. + \frac{\sin [\pi(F_{D_m} + \beta\tau)(T - |\tau|)]}{T\pi(F_{D_m} + \beta\tau)} \right] \end{aligned} \quad (34)$$

follows zero-mean complex Gaussian distributions with variance $E^2\gamma^2 [\sum_{i=1, i \neq m}^M \operatorname{sinc}^2[\pi(i - m + F_{D_i} T)] + \sin^2[\pi(F_{D_m} + \beta\tau)(T - |\tau|)] / T\pi(F_{D_m} + \beta\tau)]^2$ for the I and Q subchannels. Since $n(u, \tau)$ also follows zero-mean Gaussian distribution, so $|Z_m(u; \tau, F_{D_1}, \dots, F_{D_M})|$ of (26) follows Rayleigh distribution. In real world, the perfect values of τ and F_{D_i} are not known in the target search phase and the mean values of τ and F_{D_i} are 0, so we just assume the parameter of this Rayleigh distribution $b = \sqrt{E^2\gamma^2 + \sigma^2}$ (when τ and F_{D_i} equal to 0).

Let $y_m \triangleq |Z_m(u; \tau, F_{D_1}, \dots, F_{D_M})|$, then

$$f(y_m) = \frac{y_m}{E^2\gamma^2 + \sigma^2} \exp\left(-\frac{y_m^2}{2(E^2\gamma^2 + \sigma^2)}\right). \quad (35)$$

The mean value of y_m is $\sqrt{\pi(E^2\gamma^2 + \sigma^2)/2}$ and the variance is $(4 - \pi)(E^2\gamma^2 + \sigma^2)/2$. The variance of signal is $(4 - \pi)E^2\gamma^2/2$ and the variance of noise is $(4 - \pi)\sigma^2/2$.

Let $\mathbf{y} \triangleq [y_1, y_2, \dots, y_M]$, then the pdf of \mathbf{y} is

$$f(\mathbf{y}) = \prod_{m=1}^M f(y_m). \quad (36)$$

Our ATR is a multiple-category hypothesis testing problem, that is, to decide a target category (e.g., different aircraft, motor vehicle, etc.) based on $r_1(u, t)$. Assume there are totally N categories and category n target has RCS $\alpha_n(u)$ (with variance γ_n^2), so the ML-ATR algorithm to decide a target category C can be expressed as

$$\begin{aligned} C &= \arg \max_{n=1, \dots, N} f(\mathbf{y} | \gamma = \gamma_n) \\ &= \arg \max_{n=1, \dots, N} \prod_{m=1}^M \frac{y_m}{E^2\gamma_n^2 + \sigma^2} \exp\left(-\frac{y_m^2}{2(E^2\gamma_n^2 + \sigma^2)}\right). \end{aligned} \quad (37)$$

4.2. ML-ATR for nonfluctuating targets with delay-Doppler uncertainty

In some sources, the nonfluctuating target is identified as "Swerling 0" or "Swerling 5" model [15]. For nonfluctuating target, the RCS $\alpha(u)$ is just a constant α for a given target. Observe (26), for given τ, F_{D_i} ($i = 1, \dots, M$),

$$\begin{aligned} & \sum_{i=1, i \neq m}^M \alpha(u) E \operatorname{sinc} [\pi(i - m + F_{D_i} T)] \\ & + \frac{\alpha(u) E \sin [\pi(F_{D_m} + \beta\tau)(T - |\tau|)]}{T\pi(F_{D_m} + \beta\tau)} \\ & = \alpha E \left[\sum_{i=1, i \neq m}^M \operatorname{sinc} [\pi(i - m + F_{D_i} T)] \right. \\ & \quad \left. + \frac{\sin [\pi(F_{D_m} + \beta\tau)(T - |\tau|)]}{T\pi(F_{D_m} + \beta\tau)} \right] \end{aligned} \quad (38)$$

is just a constant. Since $n(u, \tau)$ follows zero-mean Gaussian distribution, so $|Z_m(u; \tau, F_{D_1}, \dots, F_{D_M})|$ of (26) follows

TABLE 1: RCS values at microwave frequency for 6 targets.

Index n	Target	RCS
1	Small single-engine aircraft	1
2	Large fighter aircraft	6
3	Medium bomber or jet airliner	20
4	Large bomber or jet airliner	40
5	Jumbo jet	100
6	Pickup truck	200

Rician distribution with direct path value

$$\lambda = \alpha E \left[\sum_{i=1, i \neq m}^M \operatorname{sinc} [\pi(i - m + F_{D_i} T)] + \frac{\sin [\pi(F_{D_m} + \beta\tau)(T - |\tau|)]}{T\pi(F_{D_m} + \beta\tau)} \right]. \quad (39)$$

Since τ and F_{D_i} are uncertain and zero-mean, so we just use the approximation

$$\lambda = \alpha E \quad (40)$$

which is obtained when τ and F_{D_i} equal to 0.

Let $y_m \triangleq |Z_m(u; \tau, F_{D_1}, \dots, F_{D_M})|$, then the probability density function (pdf) of y_m is

$$f(y_m) = \frac{2y_m}{\sigma^2} \exp \left[-\frac{(y_m^2 + \lambda^2)}{\sigma^2} \right] I_0 \left(\frac{2\lambda y_m}{\sigma^2} \right), \quad (41)$$

where σ^2 is the noise power (with I and Q subchannel power $\sigma^2/2$), and $I_0(\cdot)$ is the zero-order modified Bessel function of the first kind. Let $\mathbf{y} \triangleq [y_1, y_2, \dots, y_M]$, then the pdf of \mathbf{y} is

$$f(\mathbf{y}) = \prod_{m=1}^M f(y_m). \quad (42)$$

The ML-ATR algorithm to decide a target category C based on \mathbf{y} can be expressed as,

$$\begin{aligned} C &= \arg \max_{n=1, \dots, N} f(\mathbf{y} | \lambda = E | \alpha_n |) \\ &= \arg \max_{n=1, \dots, N} \prod_{m=1}^M \frac{2y_m}{\sigma^2} \\ &\quad \times \exp \left[-\frac{(y_m^2 + E^2 \alpha_n^2)}{\sigma^2} \right] I_0 \left(\frac{2E | \alpha_n | y_m}{\sigma^2} \right). \end{aligned} \quad (43)$$

5. SIMULATIONS

Radar sensor networks will be required to detect a broad range of target classes. In this paper, we applied our ML-ATR to automatic target recognition with delay-Doppler uncertainty. We assume that the domain of target classes is known a priori (N in Sections 4.1 and 4.2), and that the RSN is confined to work only on the known domain.

For fluctuating target recognition, our targets have 6 classes with different RCS values, which are summarized in Table 1 [7]. We assume the fluctuating targets follow ‘‘Swering 2’’ model (Rayleigh with pulse-to-pulse decorrelation), and assume the RCS value listed in Table 1 to be the standard deviation (std) γ_n of RCS $\alpha_n(u)$ for target n . We applied the ML-ATR algorithm in Section 4.1 (for fluctuating target case) for target recognition within the six targets domain. We chose $T = 0.1$ ms and $\beta = 10^6$. At each average SNR value, we ran Monte-Carlo simulations for 10^5 times for each target. In Figures 2(a), 2(b), 2(c), we plot the average ATR error for fluctuating targets with different delay-Doppler uncertainty and compared the performances of single-radar system, 5-radar RSN, and 10-radar RSN. Observe these three figures.

(1) The two RSNs vastly reduce the ATR error comparing to a single-radar system in ATR with delay-Doppler uncertainty, for example, the 10-radar RSN can achieve ATR error 2% comparing against the single-radar system with ATR error 37% at SNR = 32 dB with delay-Doppler uncertainty $\tau \in [-0.1 T, 0.1 T]$ and $F_{D_i} \in [-200 \text{ Hz}, 200 \text{ Hz}]$.

(2) Our LFM waveform design can tolerate reasonable delay-Doppler uncertainty which are testified by Figures 2(b), 2(c).

(3) According to Skolnik [7], radar performance with probability of recognition error (p_e) less than 10% is good enough. Our 10-radar RSN with waveform diversity can have probability of ATR error much less than 10% for the average ATR for all targets. However, the single-radar system has probability of ATR error much higher than 10%. Our RSN with waveform diversity is very promising to be used for real-world ATR.

(4) Observe Figures 2(a), 2(c), the average probability of ATR error in Figure 2(c) is not as sensitive to the SNR as that in Figure 2(a), that is, ATR error curve slope becomes flat with higher delay-Doppler uncertainty, which means that the delay-Doppler uncertainty can dominate the ATR performance when it is too high.

For nonfluctuating target recognition, our targets have 6 classes with different RCS values, which are summarized in Table 1 [7]. We applied the ML-ATR algorithms in Section 4.2 (for nonfluctuating target case) to classify an unknown target as one of these 6 target classes. We chose $T = 0.1$ ms and $\beta = 10^6$. At each average SNR value, we ran Monte-Carlo simulations for 10^5 times for each target. In Figures 3(a), 3(b), 3(c), we plotted the probability of ATR error with different delay-Doppler uncertainty. Observe these figures.

(1) The two RSNs tremendously reduce the ATR error comparing to a single-radar system in ATR with delay-Doppler uncertainty, for example, the 10-radar RSN can achieve ATR error 9% comparing against the single-radar system with ATR error 22% at SNR = 22 dB with delay-Doppler uncertainty $\tau \in [-0.2T, 0.2T]$ and $F_{D_i} \in [-500 \text{ Hz}, 500 \text{ Hz}]$.

(2) Comparing Figures 2(a), 2(b), 2(c) against Figures 3(a), 3(b), 3(c), the gain of 10-radar RSN for fluctuating target recognition is much larger than that for nonfluctuating

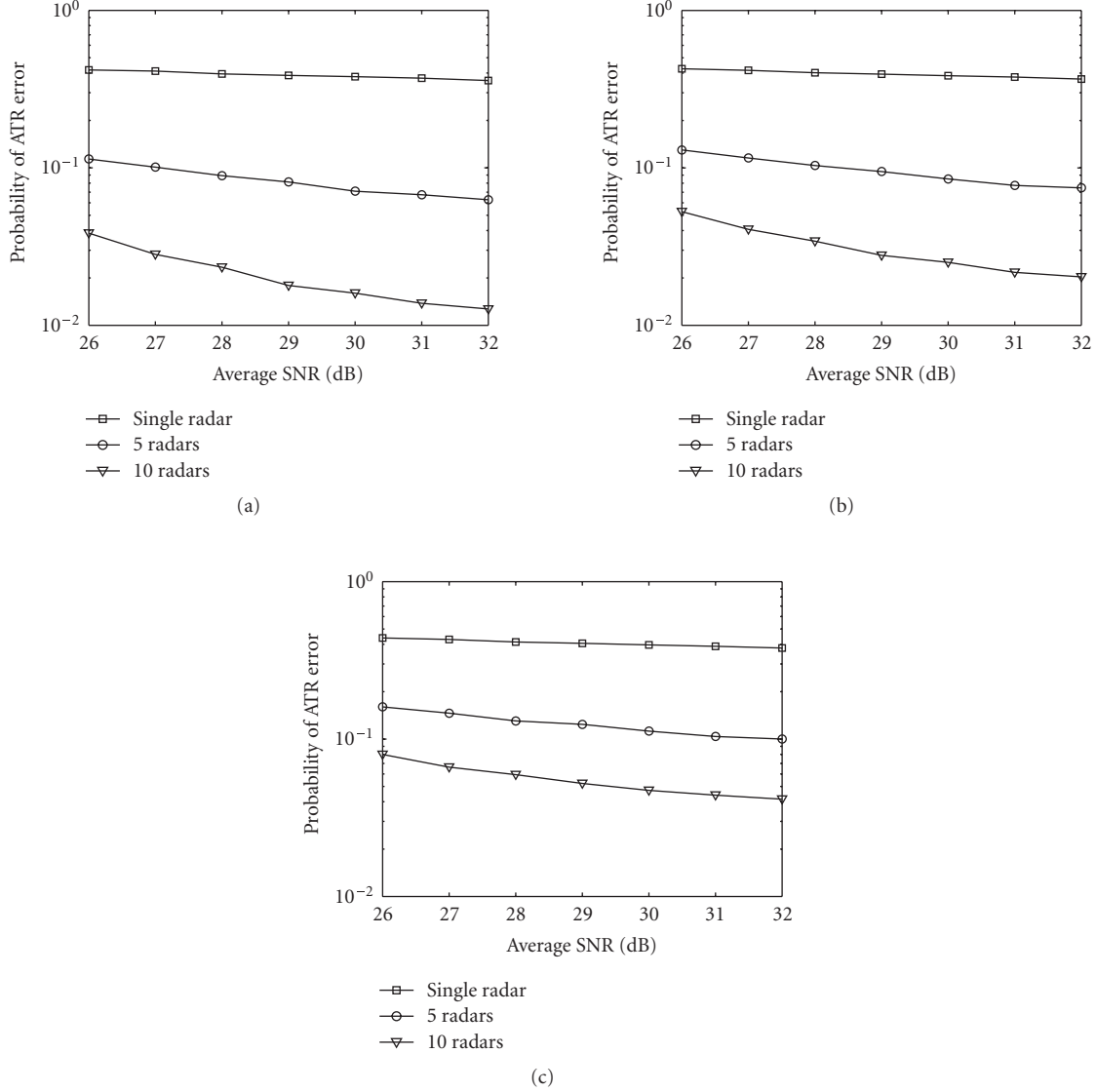


FIGURE 2: The average probability of ATR error for 6 *fluctuating* targets with different delay-Doppler uncertainty: (a) no delay-Doppler uncertainty, (b) with delay-Doppler uncertainty, $\tau \in [-0.1T, 0.1T]$ and $F_{D_i} \in [-200 \text{ Hz}, 200 \text{ Hz}]$, and (c) with delay-Doppler uncertainty, $\tau \in [-0.2T, 0.2T]$ and $F_{D_i} \in [-500 \text{ Hz}, 500 \text{ Hz}]$.

target recognition, which means our RSN has better capacity to handle the fluctuating targets. In real world, fluctuating targets are more meaningful and realistic.

(3) Comparing Figures 3(a), 3(b), 3(c) against Figures 2(a), 2(b), 2(c), the ATR needs much lower SNR for nonfluctuating target recognition because Rician distribution has direct path component.

6. CONCLUSIONS AND FUTURE WORKS

We have studied LFM waveform design and diversity in radar sensor networks (RSN). We showed that the LFM waveforms can coexist if the carrier frequency spacing is $1/T$ between two radar waveforms. We made analysis on interferences among waveforms in RSN and proposed a

RAKE structure for waveform diversity combining in RSN. We applied the RSN to automatic target recognition (ATR) with delay-Doppler uncertainty and proposed maximum-likelihood (ML)-ATR algorithms for fluctuating targets and nonfluctuating targets. Simulation results show that RSN using our waveform diversity-based ML-ATR algorithm performs much better than single-radar system for fluctuating targets and nonfluctuating targets recognition. It is also demonstrated that our LFM waveform-based RSN can handle the delay-Doppler uncertainty which quite often happens for ATR in target search phase.

The waveform design and diversity algorithms proposed in this paper can also be applied to active RFID sensor networks and underwater acoustic sensor networks because LFM waveforms can also be used by these active sensor

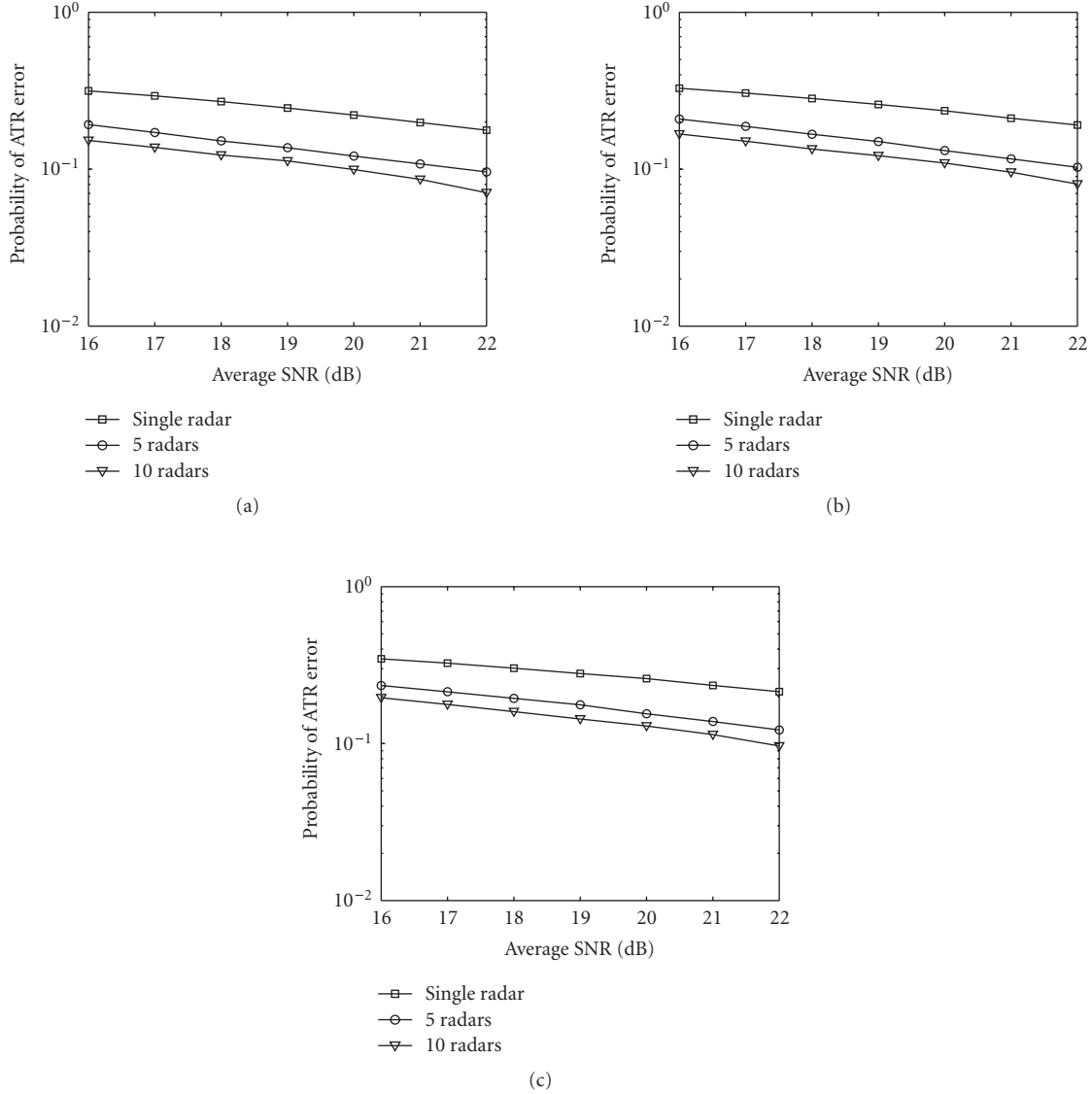


FIGURE 3: The average probability of ATR error for 6 *nonfluctuating* targets with different delay-Doppler uncertainty: (a) no delay-Doppler uncertainty, (b) with delay-Doppler uncertainty, $\tau \in [-0.1 \text{ T}, 0.1 \text{ T}]$ and $F_{D_i} \in [-200 \text{ Hz}, 200 \text{ Hz}]$, and (c) with delay-Doppler uncertainty, $\tau \in [-0.2 \text{ T}, 0.2 \text{ T}]$ and $F_{D_i} \in [-500 \text{ Hz}, 500 \text{ Hz}]$.

networks to perform collaborative monitoring tasks. In this paper, the ATR is for single-target recognition. We will continuously investigate the ATR when multiple targets coexist in RSN and each target has delay-Doppler uncertainty. In our waveform diversity combining, we have used spatial-temporal-frequency combining for RSN waveform diversity.

ACKNOWLEDGMENTS

This work was supported by the US Office of Naval Research (ONR) Young Investigator Program Award under Grant no. N00014-03-1-0466. The author would like to thank ONR Program Officer Dr. Rabinder N. Madan for his direction and insightful discussion on radar sensor networks.

REFERENCES

- [1] R. A. Johnson and E. L. Titlebaum, "Range-doppler uncoupling in the doppler tolerant bat signal," in *Proceedings of IEEE Ultrasonics Symposium*, pp. 64–67, Boston, Mass, USA, October 1972.
- [2] S. M. Sowelam and A. H. Tewfik, "Waveform selection in radar target classification," *IEEE Transactions on Information Theory*, vol. 46, no. 3, pp. 1014–1029, 2000.
- [3] P. M. Baggenstoss, "Adaptive pulselength correction (APLE-CORR): a strategy for waveform optimization in ultrawideband active sonar," *IEEE Journal of Oceanic Engineering*, vol. 23, no. 1, pp. 1–11, 1998.
- [4] D. J. Kershaw and R. J. Evans, "Optimal waveform selection for tracking systems," *IEEE Transactions on Information Theory*, vol. 40, no. 5, pp. 1536–1550, 1994.

- [5] R. Niu, P. Willett, and Y. Bar-Shalom, "Tracking considerations in selection of radar waveform for range and range-rate measurements," *IEEE Transactions on Aerospace and Electronic Systems*, vol. 38, no. 2, pp. 467–487, 2002.
- [6] Y. Sun, P. Willett, and R. Lynch, "Waveform fusion in sonar signal processing," *IEEE Transactions on Aerospace and Electronic Systems*, vol. 40, no. 2, pp. 462–477, 2004.
- [7] M. I. Skolnik, *Introduction to Radar Systems*, McGraw Hill, New York, NY, USA, 3rd edition, 2001.
- [8] H. Deng, "Synthesis of binary sequences with good autocorrelation and cross-correlation properties by simulated annealing," *IEEE Transactions on Aerospace and Electronic Systems*, vol. 32, no. 1, pp. 98–107, 1996.
- [9] Q. Liang, "Waveform design and diversity in radar sensor networks: theoretical analysis and application to automatic target recognition," in *Proceedings of International Workshop on Wireless Ad Hoc and Sensor Networks (IWVAN '06)*, New York, NY, USA, June 2006.
- [10] M. A. Richards, *Fundamentals of Radar Signal Processing*, McGraw-Hill, New York, NY, USA, 2005.
- [11] C. R. Lin and M. Gerla, "Adaptive clustering for mobile wireless networks," *IEEE Journal on Selected Areas in Communications*, vol. 15, no. 7, pp. 1265–1275, 1997.
- [12] A. Iwata, C.-C. Chiang, G. Pei, M. Gerla, and T.-W. Chen, "Scalable routing strategies for ad hoc wireless networks," *IEEE Journal on Selected Areas in Communications*, vol. 17, no. 8, pp. 1369–1379, 1999.
- [13] T.-C. Hou and T.-J. Tsai, "An access-based clustering protocol for multihop wireless ad hoc networks," *IEEE Journal on Selected Areas in Communications*, vol. 19, no. 7, pp. 1201–1210, 2001.
- [14] M. Steenstrup, "Cluster-based networks," in *Ad Hoc Networking*, C. Perkins, Ed., chapter 4, pp. 75–138, Addison-Wesley, Reading, Mass, USA, 2001.
- [15] P. Swerling, "Probability of detection for fluctuating targets," *IEEE Transactions on Information Theory*, vol. 6, no. 2, pp. 269–308, 1960.